

[Electronic Supplementary Information]

Tuning the Interparticle Distance in Nanoparticle Assemblies in Suspension via DNA-Triplex Formation: Correlation Between Plasmonic and Surface-enhanced Raman Scattering Responses

*Luca Guerrini, Fiona McKenzie, Alastair W. Wark, Karen Faulds and Duncan Graham**

Centre for Molecular Nanometrology

WestCHEM, Pure and Applied Chemistry

University of Strathclyde, 295 Cathedral Street, Glasgow, G1 1XL (UK).

E-mail: duncan.graham@strath.ac.uk

Fax: +44 141 552 0876

Tel: +44 141 548 4701

Oligonucleotides and DNA duplexes for Triplex formation

Melting curves of the triplex-to-duplex transition for oligo-functionalized NPs in the presence of dsDNA of different lengths are shown in Figure S1, whereas UV-absorption melting curves of the pure double stranded DNAs are presented in Figure S2.

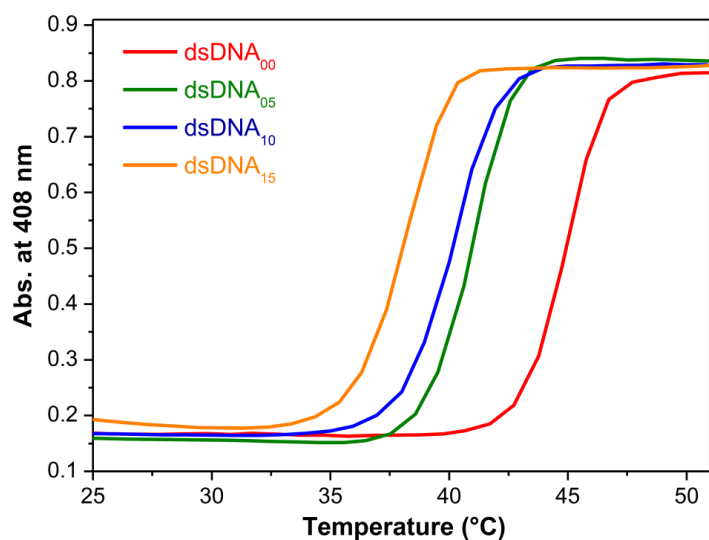


Figure S1. Triplex-to-duplex melting transitions of oligo-modified NPs for target dsDNA of different lengths. Melting experiments were recorded at 408 nm and at a heat/cool rate of 0.3 °C/minute. The melting curves indicate a sharp melting transition occurring at increasing temperatures as the dsDNA length is progressively decreased ($T_m \sim 44^\circ$, 41° , 40° and 38°C for dsDNA₀₀, ₀₅, ₁₀ and ₁₅, respectively).

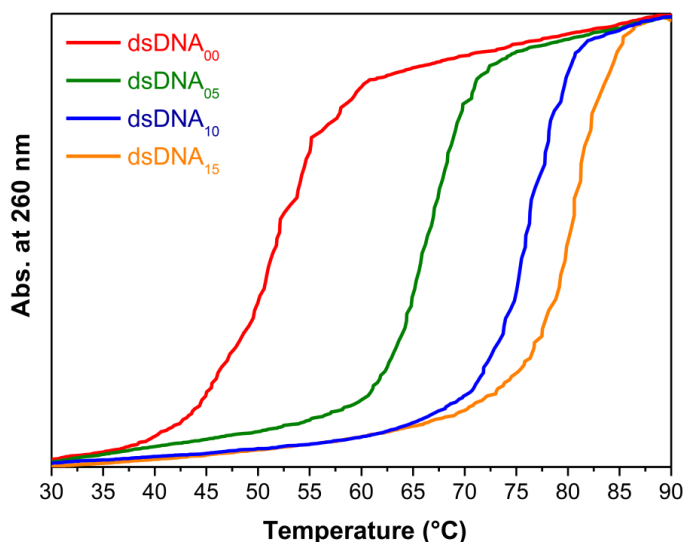


Figure S2. Duplex-to-single stranded transition of dsDNA. Normalized melting curves of dsDNA of different lengths. Melting experiments were recorded at 260 nm and at a heat/cool rate of 1 °C/minute. Melting transitions take place at higher temperatures for larger dsDNA lengths ($T_m \sim 51^\circ$, 67° , 76° and 81°C for dsDNA₀₀, ₀₅, ₁₀ and ₁₅, respectively).

Difference extinction spectra analysis

The extended broadening of the extinction spectra observed in Figure 2A of the main paper is the result of the superimposition of characteristic multi-peaked plasmonic contributions of individual NPs and clusters composed of an undefined number of randomly orientations¹ but with well-defined interparticle spacing directly related to the dsDNA length. Theoretical calculations (e.g. see Refs²⁻⁴) indicate that red-shifted resonances obtained on cluster formation are determined by the coupling of the LSPR at the interparticle gap are also highly sensitive to the excitation geometry (when the incident light is polarized). Weaker and broader “gap-plasmon” contributions emerge compared to resonances associated with single nanoparticles. To obtain further insight into the resonance contributions associated specifically with aggregation we analyzed the extinction spectra obtained in more detail.

Figure S3 illustrates the subtraction procedure for a typical data series monitoring the NP-DNA triplex assembly process. The intensity of the original extinction spectrum of the monodispersed NP probes (black line in [A]) is first normalized with respect to the maximum peak intensity of a spectrum acquired at a specific time during assembly. Figure S3B illustrates the resulting shape of the Δ extinction curve when the normalized spectrum for the monodispersed particles is subtracted from the data curve acquired at $t = 25$ mins (orange dashed line). The maximum intensity of the $t = 0$ spectrum is normalized with respect to values ranging from 40 to 100% of the peak intensity value of the $t = 25$ mins data spectrum. It can be clearly seen that subtracting the 100% normalized value helps to remove the contribution of monodispersed nanoparticles to the bulk spectrum of the partially aggregated colloid. This also reveals the formation of a new peak in the difference spectra associated with aggregate formation which we refer to as the “G-band”.

Figure S4A extends the analysis of the data series shown in Figure S3A with each difference extinction spectrum obtained by subtracting from each of the extinction spectra in Figure S3A the initial monodispersed spectrum (at $t=0$) which has been subsequently normalized to 100% of the maximum of each individual $t > 0$ min spectrum prior to subtraction. The evolution of the G-band as a function of time can then be profiled in terms of both peak position (Fig. S4B) and peak intensity (Fig. S4C).

The data in the main paper for Figures 3A and 5A were analyzed using a normalization value of 85%. However it can be clearly seen from compared the plots in Figure S4B and S4C, obtained at 100%

normalization, with Figures 3B and 5A respectively that the trends and relative values are identical and that the choice of normalization value does not create spectral artefacts during the data analysis.

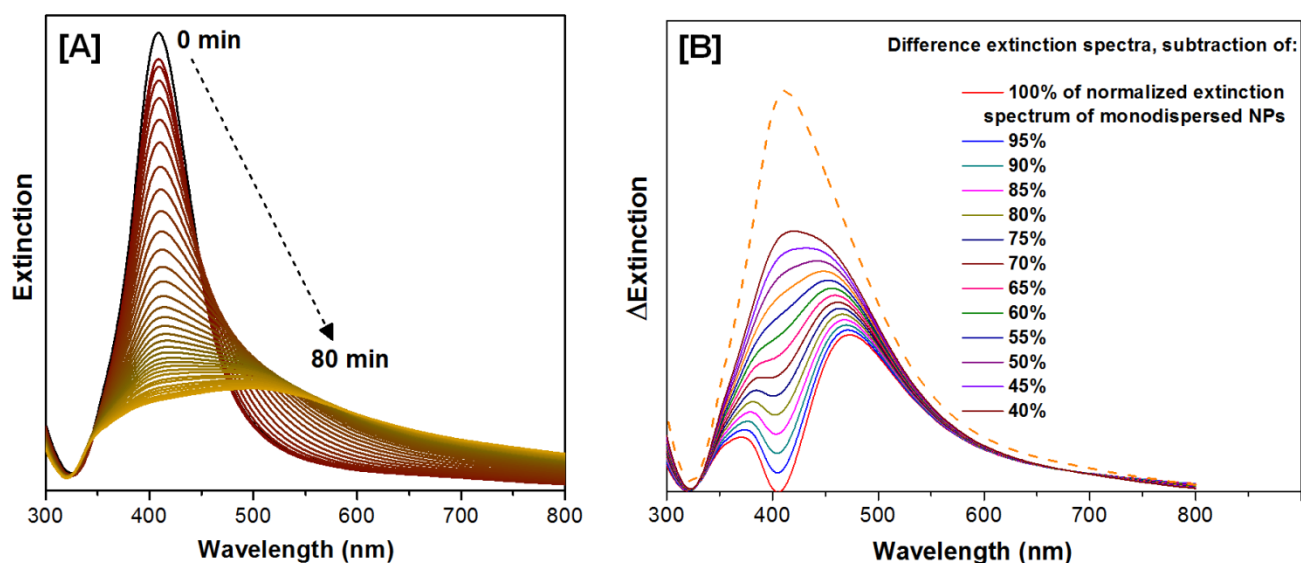


Figure S3. [A] Extinction spectra of NP probes acquired before (black line) and after the addition of complementary dsDNA₁₅ between 0-80 minutes at 150 second intervals. [B] Difference extinction spectra obtained by taking the spectrum at t = 25 mins (orange dashed line) and subtracting from this the extinction spectrum of the monodispersed NP's whose maximum value has been normalized to values ranging from 40-100% to that of the maximum of the t=25 mins spectrum.

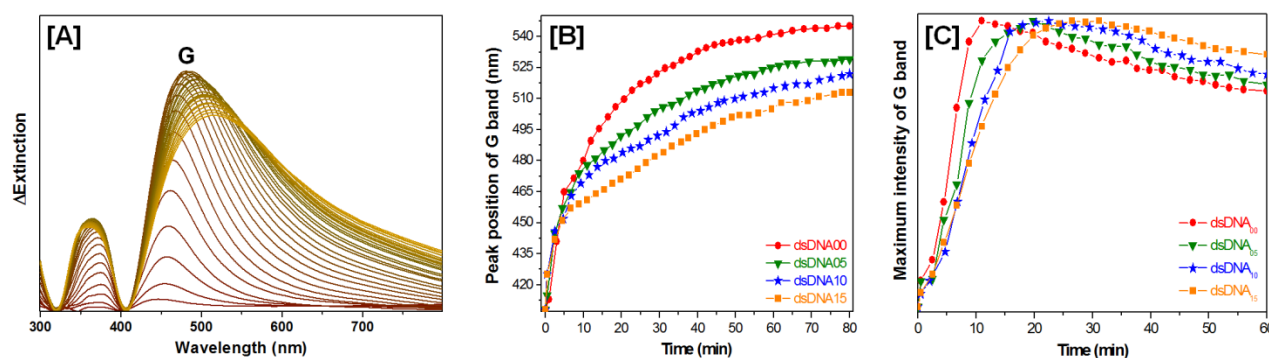


Figure S4. [A] Difference extinction spectra obtained by subtracting from each of the spectra in Figure S3A the monodispersed spectrum which has been normalized to 100% of the maximum of each individual spectrum acquired prior to subtracting. [B] Plot of “G band” peak position as a function of time for repeat measurements using lengths of target dsDNA. [C] Time dependent plot of normalized G band intensity values for each dsDNA-driven assembly. The concentrations of all the reagents were kept the same for each measurement.

Scanning electron microscope (SEM) study

To verify the information obtained from optical-based nanoparticle tracking measurements acquired during the assembly process, a series of SEM analyses were performed where the SEM substrates were immediately prepared after the extraction of sample aliquots at different times during assembly. The substrates were prepared in a humidity chamber and rinsed with water after only ~5 mins exposure to the aliquot to minimise drying-induced aggregation distorting the analysis of the cluster size distribution.

The corresponding extinction spectra at the time of the aliquot extraction alongside representative SEM images are shown in Figure S5. Figure S5A-B shows representative SEM images before the addition of dsDNA₁₅ (sample 1) with additional images corresponding to measurements at t=12 min [C-D], t=20 min [E-F], t=32 min [G-H], and t=60 min [I-L]. For each aliquot, multiple images were analysed from random areas on the substrate surface to provide a statistical evaluation of the different cluster yields with the results illustrated in Figure S5, right column. The particles were classified as monomers (M), dimers (D), trimers (Tr), tetramers (Te), pentamers (P), clusters composed of 6 to 10 nanoparticles (C₆₋₁₀), 11 to 20 nanoparticles (C₁₁₋₂₀), 21 to 50 nanoparticles (C₂₁₋₅₀) and clusters constituting more than 50 nanoparticles (C_{>50}). The results clearly indicate a trend of dynamic assembly characterized by an initial association of monomers into small clusters at the early stages of aggregation, followed by the progressive formation of larger clusters over time. It is worth noting that each of the SEM analyses at different times still indicate a significant population of monomers at each step. This agrees with the high-throughput Rayleigh-scattering imaging and tracking analysis reported in the main text which provides real-time *in situ* tracking of the cluster sub-populations. However, it is worth repeating that there is still a considerable delay between extraction of the aliquot sample and finalizing the preparation of the substrate and the effect of the substrate itself on the cluster size distribution is unpredictable.

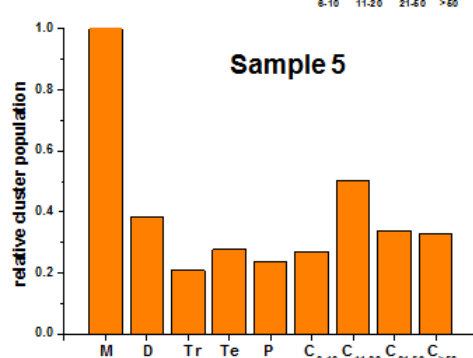
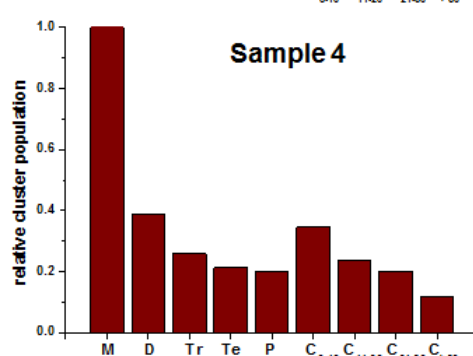
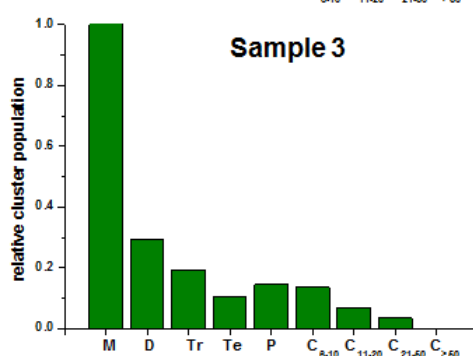
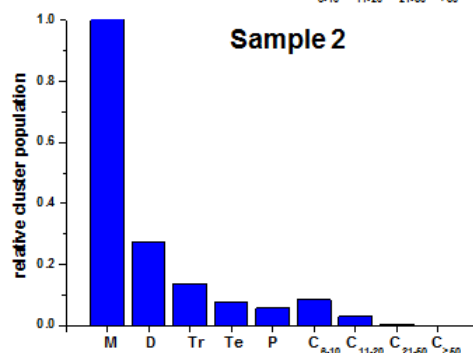
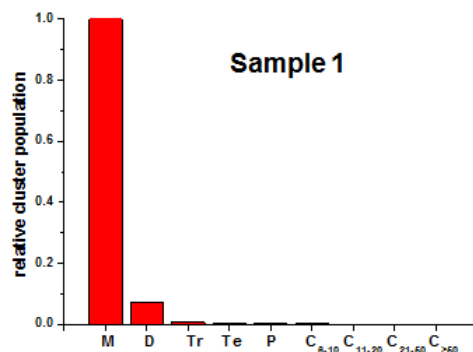
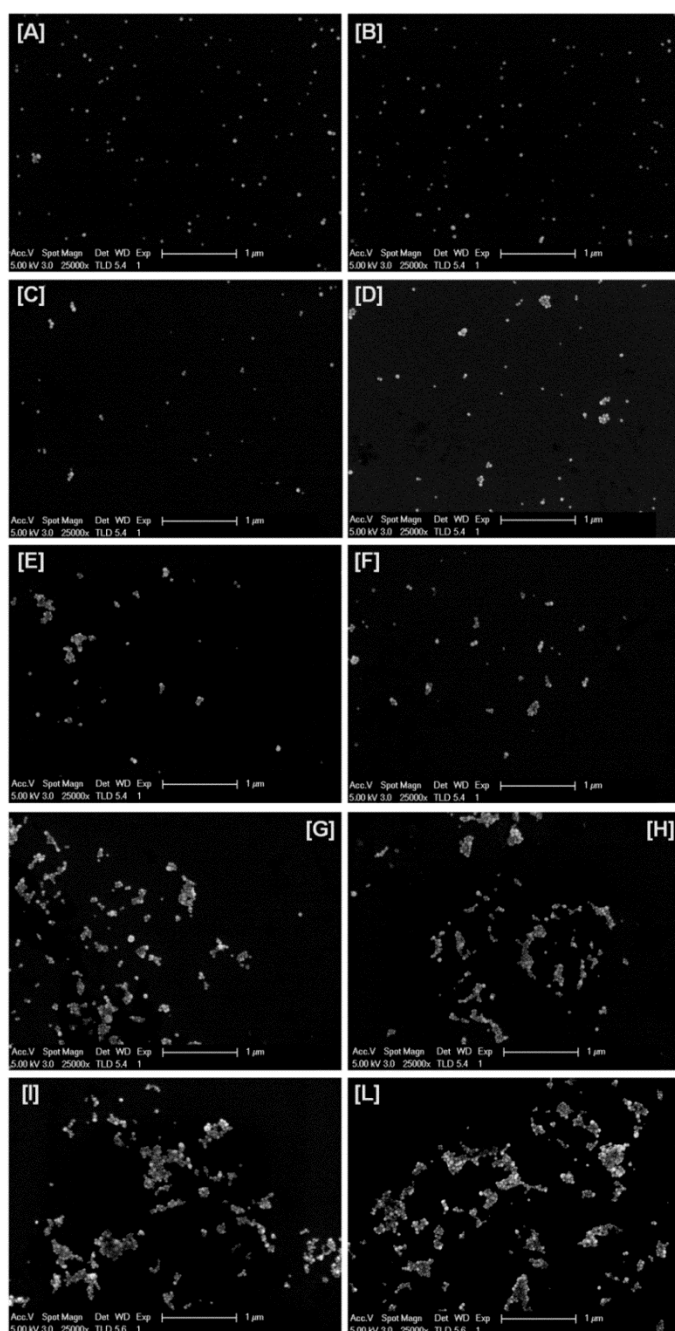
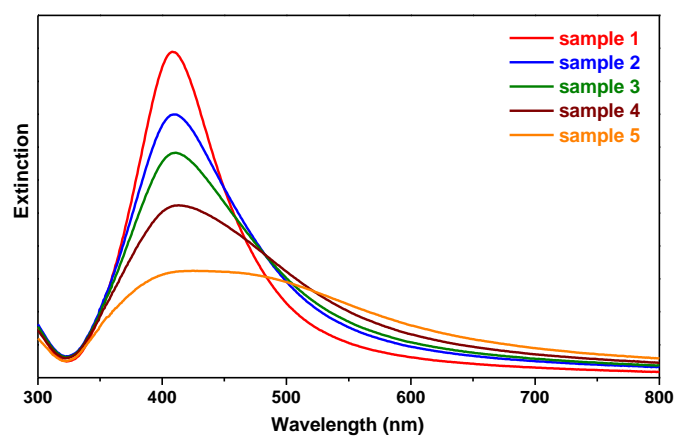


Figure S5. [Top] Extinction spectra for dsDNA15-driven NP assembly before the addition of the complementary target (sample 1) and after the addition of ssDNA at different intervals during the aggregation process (sample 2, t=12 min; sample 3, t=20 min, sample 4, t=32 min and sample 5, t=60 min). [Left column] Representative SEM images of [A-B] sample 1, [C-D] sample 2, [E-F] sample 3, [G-H] sample 4 and [I-L] sample 5 are shown. [Right column] Analysis of relative cluster population size distributions for samples 1 to 5. The statistical analyses was performed on ~1000, 700, 500, 800 and 600 individual particles/clusters for samples 1, 2, 3, 4 and 5, respectively, distributed over 15 SEM images for each sample on different areas of the wafer substrate.

References

1. N. J. Halas, S. Lal, W. S. Chang, S. Link and P. Nordlander, *Chem. Rev.*, 2011, **111**, 3913-3961.
2. E. C. Le Ru, C. Galloway and P. G. Etchegoin, *Phys. Chem. Chem. Phys.*, 2006, **8**, 3083-3087.
3. E. C. Le Ru and P. G. Etchegoin, *Principles of Surface-Enhanced Raman Spectroscopy*, Elsevier, Amsterdam, 2009.
4. E. Hao and G. C. Schatz, *J. Chem. Phys.*, 2004, **120**, 357-366.